Phylogeny, morphology, virulence, ecology, and host range of *Ordospora pajunii* (Ordosporidae), a microsporidian symbiont of *Daphnia* spp.

Marcin K. Dziuba[1,*], Kristina M. McIntire[1], Kensuke Seto[1,2], Elizabeth S. Davenport[1], Mary A. Rogalski[1,3], Camden D. Gowler[1], Emma Baird[1], Megan Vandraager[1], Cristian Huerta[1], Riley Jaye[1], Fiona E. Corcoran[1], Alicia Withrow[4], Steven Ahrendt[5], Asaf Salamov[5], Matt Nolan[5], Sravanthi Tejomurthula[5], Kerrie Barry[5], Igor V. Grigoriev[5,6], Timothy Y. James[1], and Meghan A. Duffy[1]

Affiliations

[1] Department of Ecology & Evolutionary Biology, University of Michigan, Ann Arbor, MI 48109, USA

[2] Faculty of Environment and Information Sciences, Yokohama National University, Yokohama, Kanagawa, 240□8502, Japan

[3] Biology Department, Bowdoin College, Brunswick, ME 04011, USA

[4] Center for Advanced Microscopy, Michigan State University, East Lansing, MI, 48824 USA

[5] United States Department of Energy Joint Genome Institute, Lawrence Berkeley National Laboratory, Berkeley, CA, USA

[6] Department of Plant and Microbial Biology, University of California Berkeley, Berkeley, CA, USA

[*] Correspondence: marcind@umich.edu; marcinkdziuba@gmail.com

Running Title

O. pajunii - a symbiont of *Daphnia*

Data Availability

Life table and lake prevalence data will be deposited to a public database such as Dryad upon acceptance of the manuscript. The genetic data has been deposited in GenBank.

Abstract

Symbiosis is increasingly recognized as a dynamic relationship, with the net outcome falling along a continuum from mutualism to parasitism. A key example of this comes from a recently discovered microsporidian symbiont of *Daphnia,* the net impact of which was found to vary from negative to positive. We investigated the taxonomic position of this microsporidian and the morphology of infected hosts, as well as the virulence, ecology and host range of the symbiont; we also provide information about its culturing methods. The genetic data indicates that the microsporidian symbiont belongs to *Ordospora pajunii*, a newly described microsporidian parasite of *Daphnia*. We show that *O. pajunii* infection damages the gut, causing infected epithelial cells to lose microvilli and then rupture. The prevalence of this microsporidian can be

high (up to 100% in the lab and 77% of adults in the field). Its overall virulence seems low in most cases, but some genotypes suffer reduced survival and reproduction. Susceptibility and virulence are strongly host-genotype dependent. We found that North American *O. pajunii* are able to infect multiple *Daphnia* species, including the European species *D. longispina*, as well as the genus *Ceriodaphnia*. We propose the *Daphnia* - *O. pajunii* symbiosis as a valuable system for studying the mechanisms of context-dependent shifts between mutualism and parasitism, as well as for understanding how symbionts might alter host interactions with resources.

Importance

The net outcome of symbiosis can shift between parasitism and mutualism, but the mechanisms underlying such changes remain cryptic. A full understanding of what drives shifts of symbiotic relationships will require comprehensive knowledge of the biology and ecology of the symbionts. However, we have few systems in which this is possible, especially for cases where something that is typically a parasite becomes a mutualist. Recently, a microsporidian symbiont of *Daphnia* was found to shift from parasitism towards mutualism, but little was known about this symbiont (including its species identity). Here, we describe this endosymbiont of *Daphnia*, identifying it as the microsporidium *Ordospora pajunii*. We described its phylogeny, morphology, virulence and ecology, enabling future study of this interaction as a model for shifts along the mutualism-parasitism continuum.

Keywords
Microsporidia, mutualism-parasitism continuum, symbiosis, pathogen, zooplankton

Introduction

Symbiotic interactions can vary from mutualistic to parasitic depending on the underlying ecological context, e.g.(1). Whether the net outcome of the interaction is positive (mutualism), neutral (commensalism) or negative (parasitism) is determined by the sum of the costs and benefits for both parties involved, and this sum can be altered by abiotic and biotic factors (2). Three examples help illustrate the context dependency of symbiotic relationships: the presence of a bird nest parasite (cuckoo) has negative effects on fitness of the host birds, but can sometimes yield a net benefit if the parasitic chicks repel nest predators, saving the entire nest from their attacks (3); the mutualistic relationship between the dinoflagellate *Symbiodinium* and its coral host shifts into parasitism under temperature increase, due to the increased uptake of nutrients by the former (4); and a fungal parasite of the plant *Brassica napus* becomes a mutualist when it is itself infected with mycovirus (5). While it is now clear that it is possible to move along the mutualism-parasitism continuum, examples with well-characterized mechanisms underlying this shift are still scarce, particularly for typically parasitic organisms moving towards mutualism. To understand the mechanism underlying these shifts, we need to develop additional model systems where comprehensive knowledge of symbiont biology and ecology will allow for uncovering the costs and benefits of the interaction and how these change with ecological context.

A recent study found that infection of *Daphnia dentifera* (an ecologically important zooplankton host) with an unknown microsporidian can be beneficial or harmful for the host depending on the ecological context (6). Microsporidia are obligately intracellular and have highly reduced metabolism (7); they steal ATP and nucleotides from their host, inflicting negative consequences to host fitness (8). Therefore, it was not surprising that the gut-infecting microsporidian was often found to have negative effects on *Daphnia*, especially when the host experienced food scarcity (6). However, infection with the microsporidian made the host's gut less penetrable by spores of highly virulent fungus *Metschnikowia bicuspidata*. Intriguingly, *Daphnia* infected with the microsporidium had a reproductive advantage over the non-infected individuals when *M. bicuspidata* was common. Overall, the net outcome of infection with the microsporidium spanned from parasitic through commensal to mutualistic, depending on the availability of food for the host and the prevalence of more virulent pathogens. Additionally, the effect size of infection with this microsporidian on the immune traits of *Daphnia* was found to be variable between lakes (9), which further indicates that the strength of the impact of the interaction on the host is context dependent. Thus, this *Daphnia*-microsporidium interaction has the potential to allow for better exploring the context dependency of symbiosis. However, while the host is a well-established model, with a wealth of information about its genetics, physiology and ecology (10, 11), little is known about the microsporidian. Indeed, in the prior studies showing context dependent outcomes (6, 9), it was referred to as "MicG" (because it is a microsporidian that attacks the gut), without a formal scientific name.

Here we focus on the taxonomy, morphology, virulence, host range, and ecology of this microsporidian symbiont of *Daphnia*. A very similar parasite was recently described from *Daphnia longispina* in Europe (12) and named *Ordospora pajunii*. We present sequence data from MicG from infected hosts from multiple lakes and an analysis of its full genome, with a

114 particular focus on comparing our MicG isolates with *O. pajunii*. Additionally, we provide light
115 microscopy and transmission electron microscopy images of MicG, on which we base our
116 description of the morphology and biology of infection. Moreover, we performed a lab
117 experiment investigating the effects of the microsporidian on life history parameters of its host,
118 *Daphnia dentifera*. We also provide data on the prevalence of infection in four natural *D.*
119 *dentifera* populations in the lakes of North America. Finally, we present information on the host
120 range of this microsporidium, including tests of whether MicG can infect *D. longispina* (the host
121 from which *O. pajunii* was originally described). Together, this work not only establishes the
122 identity of this intriguing symbiont, but also reveals more about its morphology, life history, and
123 ecology.
124
125 **Materials and methods**
126 *Overview*
127 During an intensive study of host-symbiont interactions (6), we noticed this microsporidian
128 infecting the guts of *Daphnia dentifera*. *Daphnia dentifera* Forbes is a dominant grazer in lake
129 food webs in stratified lakes in the Midwestern United States (13) that hosts a variety of
130 parasites (14, 15). The intensive study revealed that this microsporidian shifts along a
131 mutualism-parasitism continuum (6) and spurred the work reported in this manuscript. The data
132 on prevalence in four natural populations comes from the same field sampling as was reported
133 in Rogalski et al. (6); however, that study did not analyze the temporal dynamics of infections.
134
135 *Sequencing and phylogenetic analysis*
136 <u>SSU rRNA sequencing</u>
137 To investigate the phylogenetic affiliation of our microsporidian, we analyzed partial sequences
138 of SSU rRNA of 9 individuals of *D. dentifera* infected with MicG collected in 2021 from Crooked
139 Lake ("Crooked-W" in Table S1; Washtenaw County, Michigan, USA) and 9 individuals from
140 Walsh Lake (Washtenaw County, Michigan, USA), against the sequences available in Genbank.
141 DNA was extracted using DNeasy Blood and Tissue kit (Qiagen®). Each infected *Daphnia* was
142 picked from a microscope slide using jewelers forceps, placed in a 1.5 ml centrifuge tube with
143 100 µL and frozen until the DNA extraction was carried out. The defrosted animals were placed
144 (with forceps) in 180 µL of ATL buffer, 20 µL of Proteinase K was added to each tube, and all
145 tubes were incubated at 56°C for 24 hours. The next steps of the extraction were performed
146 following the protocol described by the producer.
147
148 We amplified the SSU sequence of MicG using primers V1F
149 (CACCAGGTTGATTCTGCCTGAC) and 530R (CCGCGGCKGCTGGCAC) (Trzebny et al.
150 2020) and KOD Xtreme™ Hot Start DNA Polymerase kit (Novagen®). The PCR was performed
151 using an initial step of 3 min at 95°C and then 35 cycles of 10 sec at 95°C followed by 30 sec at
152 60°C and 1 min at 72°C, and a final step of 5 min at 72°C. The PCR product was cleaned with
153 ExoSAP-IT™ (ThermoFisher Scientific®) kit using the manufacturer's protocol, then Sanger
154 sequenced by Eurofins Genomics® on an ABI 3730 XL Analyzer (Applied Biosystems) using
155 forward and reverse primers on each product. The sequences obtained with forward and

156 reverse primers were combined (after converting the reverse sequence into its reverse-
157 complement version) and manually corrected to eliminate any sequencing errors. The MicG
158 sequences were compared to sequences available in GenBank using blastn and the taxa
159 indicated as the most similar were used to create a phylogenetic tree. The selected sequences
160 were cropped to similar size and aligned using the ClustalW algorithm in MEGA X version
161 10.0.5 (Kumar et al. 2018). A maximum likelihood phylogenetic tree was computed in MEGA X,
162 using the Tamura 3-parameter model and 1000 bootstrap replicates.
163
164 ITS sequencing
165 Microsporidia are closely related to (or considered to be) fungi (16, 17), and the well-established
166 molecular barcode for fungi is the Internal Transcribed Spacer (ITS) sequence (18). Therefore,
167 we also analyzed ITS sequences of MicG infecting 7 *D. dentifera* from Crooked W Lake, 7 from
168 Walsh Lake, 8 *D. dentifera* clone "S" from our lab culture of MicG isolate collected from lake
169 Walsh and 1 *Daphnia mendotae* from Woodland Lake (Washtenaw County, Michigan, USA), all
170 collected in 2021. Samples from Walsh and Crooked-W sequenced for ITS were a subset of the
171 same samples as used for SSU (see above). The DNA extraction was performed using the
172 same protocol as for SSU. The amplification was performed using primers ITSF-MicG
173 (GGGGTGTGAGTCTTCTGTGG) and ITSR-MicG (GTTCAGCATCACACAACCCG) and the
174 same PCR kit as above. The PCR parameters were an initial step of 5 min at 95°C and then 35
175 cycles of 30 sec at 95°C followed by 1 min at 53°C and 2 min at 72°C, and a final step of 5 min
176 at 72°C. The product was purified with ExoSAP-IT™ and Sanger sequenced by Eurofins
177 Genomics®. The sequences were manually corrected and analyzed with the same software and
178 methods as above, except for the alignment, which was performed with the Muscle algorithm
179 and manually corrected.
180
181 Whole genome sequencing
182 We applied single cell genome sequencing techniques to sequence the MicG genome (19). A
183 single *D. dentifera* was placed on a microscope slide in a droplet of MilliQ water and her gut was
184 dissected, extruding the microsporidia. The spores were collected with a glass pasteur pipette
185 and transferred into another droplet of MilliQ water, where large host tissue particles were
186 removed. The spores were collected from the slide with a glass pipette and stored in a 1.5 mL
187 centrifuge tube. Spores were isolated using a manually prepared drawn-out glass capillary
188 pipette. A small amount (100–200 µL) of the spore suspension was transferred onto a petri dish
189 and observed under an inverted microscope. We isolated ~20 spores by pipette and put them
190 into a small drop of UV-sterilized water. From them, 5–10 spores were isolated by avoiding
191 putative contamination of host tissues and transferred into 200 µL PCR tubes with 1-2 µL of
192 water. DNA extraction and whole genome amplification were performed using the Qiagen
193 REPLI-g Single Cell kit (Qiagen, Maryland, USA). The prepared libraries were quantified using
194 KAPA Biosystems' next-generation sequencing library qPCR kit and run on a Roche LightCycler
195 480 real-time PCR instrument. Sequencing of the flowcell was performed on the Illumina
196 NovaSeq sequencer using NovaSeq XP V1.5 reagent kits, S4 flowcell, following a 2x151
197 indexed run recipe. Ten million reads were filtered for JGI process contaminants with
198 bbtools.Seal, subsampled using bbtools.reformat.sh (http://sourceforge.net/projects/bbmap),
199 and assembled using SPAdes version v3.15.3 ((20) using parameters: --phred-offset 33 --cov-

cutoff auto -t 16 -m 64 --careful -k 25,55,95). After the assembly, the scaffolds < 1000bp were removed. The genome was annotated using the JGI Annotation pipeline and shared via JGI MycoCosm (21).

Phylogenomic analysis was performed using a dataset of 40 Microsporidia taxa (Table S2). Two species of Metchnikovellidae (*Amphyamblys* sp. and *Metchnikovella incurvata*) were selected as the outgroup. The “genome mode” of BUSCO version 5 (22) was run for each microsporidian genome using the microsporidia_odb10 database. A concatenated alignment was prepared using the version 4 of “BUSCO_phylogenomics” pipeline (https://github.com/jamiemcg/BUSCO_phylogenomics, (23)). Single copy BUSCO genes present in more than 80% of 40 microsporidians (“-psc 80”) were extracted from the outputs of BUSCO. Each gene sequence was aligned with muscle v3 (Edgar 2004) and trimmed with trimAl v1.2 (24). The final concatenated alignment comprised 102,302 amino acids from 332 genes. A maximum likelihood (ML) analysis was performed using IQ-TREE v2 (25) using the site-heterogeneous model (LG + C60 + F + G + PMSF, (26)). The tree inferred using the LG + F + R9 model selected by ModelFinder (27) was used as a guide tree for PMSF model analysis. A standard nonparametric bootstrap analysis (100 replicates) was done under the LG + C60 + F + G + PMSF model.

Based on phylogenetic similarity to *Ordospora pajunii* FI-F-10, we performed comparative analyses to determine the extent of genetic differences between the genomes of *O. pajunii* and MicG. The genomes were first compared to calculate average nucleotide identity using OAT 0.93.1 with the OrthoANI algorithm (28). Alignment of FI-F-10 and MicG was conducted using Parsnp v1.2 (29) to identify single nucleotide polymorphisms (SNPs). We used SnpEff 5.0e (30) to calculate the putative function effects of the SNPs using the annotation of FI-F-10 as a reference. PRODIGAL v2.6.3 (31) was used to annotate the genome of MicG, which was then compared to FI-F-10 by OrthoFinder v. 2.5.2 (32) to identify genes that were missing or duplicated in one or the other genome assemblies.

Microscopy

We used a combination of light and transmission electron microscopy to explore the morphology of MicG, as well as the symptoms associated with infection.

<u>Light microscopy</u>

We used an Olympus DP73 camera attached to an Olympus SZX16 dissecting microscope to take photomicrographs of *D. dentifera* infected with MicG at 4 - 11.5x magnification. In addition, MicG spores were extracted by rupturing the gut of four infected *Daphnia* on a microscope slide; the length and width of 25 spores from each *Daphnia* were measured using the same camera attached to an Olympus BX53 microscope (1000x magnification) and using Olympus cellSens Imaging Software.

<u>Transmission electron microscopy</u>

243 To characterize the ultrastructure of MicG, as well as the impact on infected host cells and gut
244 morphology, we collected twenty MicG-infected *D. dentifera* individuals from lab cultures (see
245 Supplemental Materials), fixed them in 3% glutaraldehyde, and stored at 4°C for over two
246 weeks. After primary fixation, samples were washed with 0.1M phosphate buffer and postfixed
247 with 1% osmium tetroxide in 0.1M phosphate buffer, dehydrated in a gradient series of acetone
248 and infiltrated and embedded in Spurr's resin. 70 nm thin sections were obtained with a Power
249 Tome Ultramicrotome (RMC, Boeckeler Instruments, Tucson, AZ) and post stained with uranyl
250 acetate and lead citrate. Images were taken with a JEOL 1400Flash Transmission Electron
251 Microscope (Japan Electron Optics Laboratory, Japan) at an accelerating voltage of 100kV.
252
253 *Life table measures of parasite virulence*
254 To quantify parasite virulence (with respect to reproduction and lifespan), we carried out life
255 table experiments with 7 genotypes of *Daphnia dentifera* (S and A43, originally isolated from
256 lakes in Barry County, Michigan, and M37, ML32, BD08, DW29, and DW22, originally isolated
257 from lakes in Sullivan and Greene Counties, Indiana). These clones were chosen as they
258 display varied susceptibility to other pathogens (unpublished data). We first reared individuals
259 from these genotypes for 3 generations in standard conditions to standardize maternal effects.
260
261 On experiment day 1, 0-24hr old neonates were collected and placed individually into 50mL
262 beakers, with 30mL filtered lake water and 1mL standard food stock (to a final concentration of
263 ~33,000 cells/mL of *Ankistrodesmus falcatus*). Animals were assigned to one of three pathogen
264 treatments: MicG48, receiving one dose of MicG at 48 hr old and a placebo at 120 hr old;
265 MicG120, receiving a placebo at 48 hr old and one dose of MicG at 120 hr old; and Control,
266 receiving a placebo at 48 hr and 120 hr. Two exposure windows were chosen as previous
267 observations suggested MicG may more effectively infect hosts very early in the host lifespan.
268 There were 10 replicate individuals per clone * exposure treatment combination (210 individuals
269 total). Animals were housed in environmental chambers at 20°C with a 16h:8h (light:dark) cycle
270 for the duration of the experiment.
271
272 On day 2, all animals were transferred to new beakers with 10mL filtered lake water and given
273 either a dose of MicG or a placebo. For MicG doses, a slurry was created by crushing *Daphnia*
274 *dentifera* (S clone, in which we cultivate this symbiont) with high MicG infectious burden into
275 10mL MilliQ water; this slurry contained a ratio of 1 high burden donor: 1 experimental animal,
276 with each experimental animal exposed to a portion of the slurry equivalent to 1 high burden
277 donor (e.g., if 10 animals were being exposed, the slurry would be created using 10 highly
278 infected donors, and each experimental animal would receive 1/10th of the resulting slurry). The
279 placebo was created and dosed in the same manner, using uninfected animals. After 48 hours,
280 animals were moved to new, parasite-free beakers with 30mL filtered lake water. On day 5, the
281 exposure treatment was repeated as above; this time, animals in the MicG120 treatment
282 received the spore slurry and the other two treatments received the placebo. During exposure,
283 animals were given 0.5mL stock food per day, all other experimental days animals received
284 1mL stock food daily (1,000,000 *A. falcatus* cells/mL in the stock food solution).
285

286 We checked animals daily for mortality and offspring production. We recorded the date and
287 number of offspring produced (offspring were removed from the beaker) as well as the date of
288 death. Animals were checked for infection twice per week under the dissecting microscope (4-
289 10x magnification).
290
291 We calculated the proportion of exposed hosts that became infected for each genotype and
292 infection timing combination. We then tested for effects of the parasite and timing of parasite
293 exposure on host life history traits. We used an aligned rank ANOVA to analyze total fecundity,
294 a generalized linear model (GLM) to analyze body size at first reproduction, and a proportional
295 hazard model stratified by genotype to analyze time to death. These analyses were restricted to
296 the four genotypes that displayed substantial infection (BD08, DW29, DW22 and S). The
297 analyses included all individuals in a genotype*treatment combination; results were not
298 qualitatively different if only infected individuals were included for the MicG48 and MicG120
299 treatments.
300
301 *Prevalence in natural populations*
302 We sampled four lake populations in Southeastern Michigan in 2016: Gosling Lake in Livingston
303 County and North, Pickerel, and Sullivan Lakes in Washtenaw County (Table S1). These lakes
304 were sampled every three days from late July through mid-November. This sampling window
305 was chosen because outbreaks of other *D. dentifera* parasites occur primarily in late summer
306 and autumn (33, 34). Each lake was sampled by taking whole water column tows with a
307 Wisconsin net from three locations in the deep basin of the lake. These three tows were pooled,
308 and then a subsample was analyzed to determine the prevalence of individuals that were
309 infected; this was done by examining each individual in the subsample under a dissecting
310 microscope at 40-50x using dark field microscopy, looking for characteristic signs of infection
311 along the gut (described more below). We aimed to have at least 200 *D. dentifera* individuals in
312 the subsample that was analyzed for infections; if there were fewer than 200 individuals in the
313 whole sample, we analyzed the entire sample. Over the entire study period, the median number
314 of *D. dentifera* that we analyzed for infection was 233.5 per lake-day combination (mean: 236,
315 minimum: 71, maximum: 449). Because adults are more likely to have visible signs of infection,
316 we focus on the proportion of the adult population that was infected in our analysis.
317
318 *Host range*
319 We used a dataset from 15 inland lakes in Southeastern Michigan collected in 2021 to assess
320 which *Daphnia* species are infected by MicG in natural populations. The 15 lakes are the same
321 as those in Gowler et al. (35); more information about each can be found in Table S1.
322
323 To check whether MicG can infect European *D. longispina* (the host from which *O. pajunii* was
324 described), we exposed five clones of *D. longispina* collected from three German lakes, along
325 with the *D. dentifera* clone S (used as a control for infection success) to MicG spores. We
326 synchronized the mothers of experimental animals, and reared them until they gave birth to their
327 first clutch. The first clutch babies were harvested within 24 h of birth and placed singly in a 50
328 mL beaker filled with 20 mL of filtered lake water and fed 0.5 mL of a standard food stock
329 (1,000,000 *A. falcatus* cells/mL in the stock food solution) daily until the end of exposure. We

330 exposed 10 individuals from each of the 6 clones. After 48 h, all animals were dosed with a
331 MicG spore slurry; each animal was exposed to a spore suspension equivalent to one donor
332 individual, similar to the approach used in the life table experiment above. Exposure lasted 48 h,
333 after which we transferred *Daphnia* to new beakers filled with 40 mL of filtered lake water, fed
334 them 1 mL of stock food daily and checked for mortality until the end of the experiment. We
335 initially checked *Daphnia* for infection under the dissecting microscope 7 days after exposure,
336 then checked them twice a week thereafter. The experiment ended on day 30. The S clone
337 individuals that we used as a positive control had 100% MicG infection prevalence in this trial.
338
339 **Results**
340 *Sequencing and phylogenetic analysis*
341 The SSU and ITS sequences of MicG suggest a very close affinity with *Ordospora pajunii*
342 (Figure 1), a microsporidian species recently described from *Daphnia longispina* in Finland (12).
343 Moreover, there was no variation within the MicG isolates at SSU or ITS, and very little between
344 MicG and the published sequences of *O. pajunii* (Figure 1A,B). There was a clear separation
345 from the *Ordospora colligata* clade, however, at both loci.
346
347 We assembled the MicG genome into 42 contigs of total length 2.24 Mb with a contig n50 of 133
348 kb. A phylogenomic analysis using the amino acid sequences of 332 genes corroborated the
349 high genetic similarity of MicG to *O. pajunii* (Figure 1C). The average nucleotide identity
350 between MicG and *O. pajunii* was 99.84%, which is well within the 95% limit recently suggested
351 for species (12). The MicG genome annotation revealed 1946 protein coding genes. Alignment
352 of the MicG and *O. pajunii* genomes uncovered 2,666 SNPs and 1,004 bp associated with
353 indels differing between the strains. 12.8% of the SNPs were intergenic, and, of the SNPs in
354 exons, 55.3% were missense, and 8 total nonsense SNPs were observed. Comparison of the
355 two largest contigs of MicG to *O. pajunii* revealed colinearity of chromosomes (Figure 2), with
356 most of the variation between the two genomes appearing at the ends of contigs. High variability
357 of the genome in the subtelomeric regions with associated repeat regions and a ribosomal RNA
358 gene array is also observed for other microsporidia (36). Ribosomal RNA, however, was not
359 associated with the ends of contigs in *O. pajunii* or MicG and mostly absent from the genome
360 assemblies save one small contig in each genome, suggesting our assemblies are incomplete
361 towards the telomeres. Beyond the subtelomeric regions, we inspected genes with the highest
362 number of amino acid changing SNPs between the strains. The highest number of missense
363 mutations (Figure S1) were in: an alpha/beta hydrolase (20 SNPs; *O. pajuni* protein accession
364 number: KAH9410807.1), a hypothetical protein (11 SNPs; KAH9411254.1), a DEAD/DEAH box
365 helicase (7 SNPs; KAH9411242.1), and an aminopeptidase (7 SNPs; KAH9410533.1). There
366 was no evidence for genes present in one strain but not the other when only considering the
367 large contigs (>10 kb).

368

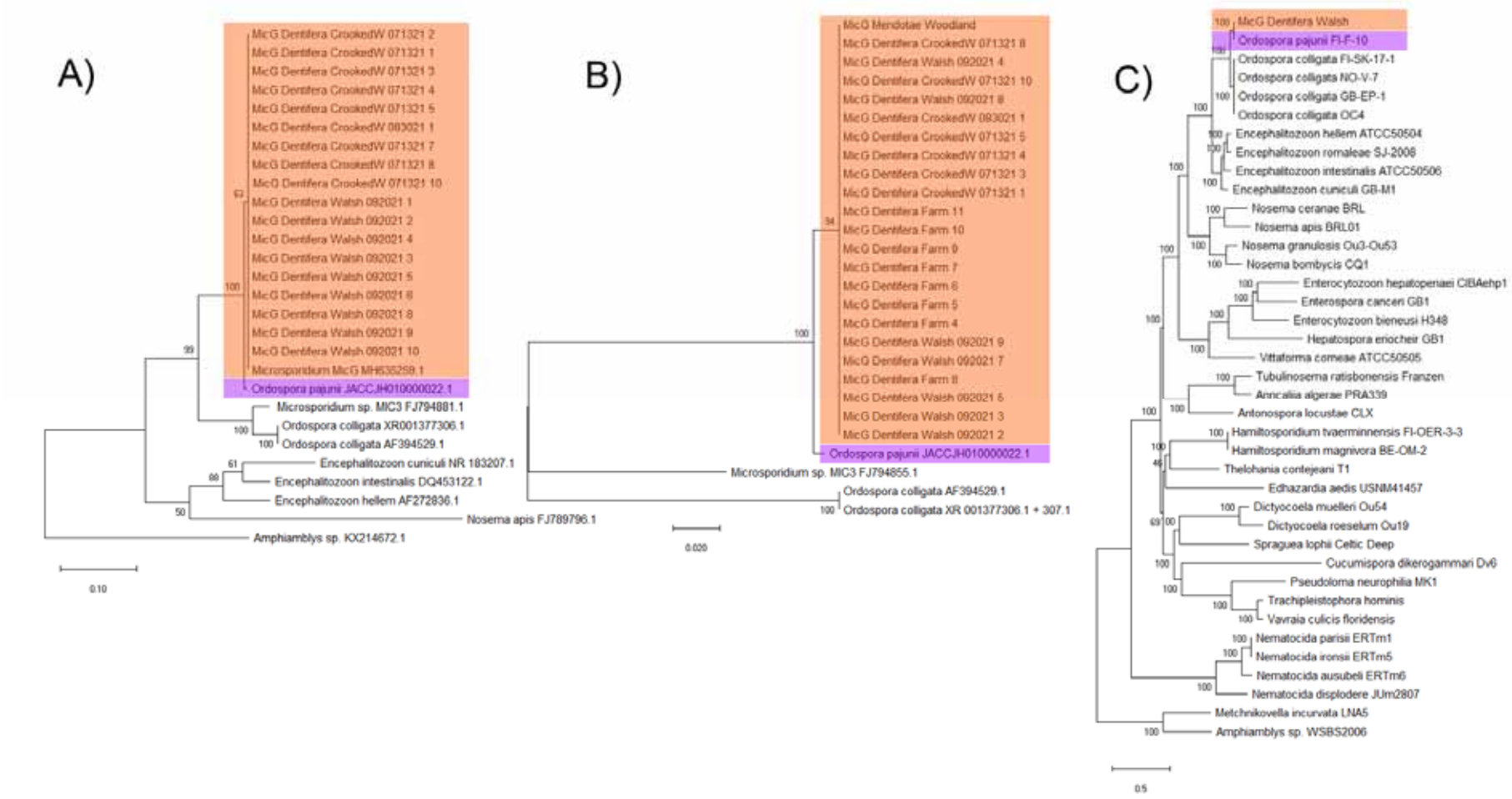
A)
MicG Dentifera CrookedW 071321 2
MicG Dentifera CrookedW 071321 1
MicG Dentifera CrookedW 071321 3
MicG Dentifera CrookedW 071321 4
MicG Dentifera CrookedW 071321 5
MicG Dentifera CrookedW 083021 1
MicG Dentifera CrookedW 071321 7
MicG Dentifera CrookedW 071321 8
MicG Dentifera CrookedW 071321 10
MicG Dentifera Walsh 092021 1
MicG Dentifera Walsh 092021 2
MicG Dentifera Walsh 092021 4
MicG Dentifera Walsh 092021 3
MicG Dentifera Walsh 092021 5
MicG Dentifera Walsh 092021 6
MicG Dentifera Walsh 092021 8
MicG Dentifera Walsh 092021 9
MicG Dentifera Walsh 092021 10
Microsporidium MicG MH636259.1
Ordospora pajunii JACCJH010000022.1
Microsporidium sp. MIC3 FJ794881.1
Ordospora colligata XR001377306.1
Ordospora colligata AF394529.1
Encephalitozoon cuniculi NR 183207.1
Encephalitozoon intestinalis DQ453122.1
Encephalitozoon hellem AF272836.1
Nosema apis FJ789796.1
Amphiamblys sp. KX214672.1
0.10
B)
MicG Mendotae Woodland
MicG Dentifera CrookedW 071321 8
MicG Dentifera Walsh 092021 4
MicG Dentifera CrookedW 071321 10
MicG Dentifera Walsh 092021 8
MicG Dentifera CrookedW 083021 1
MicG Dentifera CrookedW 071321 5
MicG Dentifera CrookedW 071321 4
MicG Dentifera CrookedW 071321 3
MicG Dentifera CrookedW 071321 1
MicG Dentifera Farm 11
MicG Dentifera Farm 10
MicG Dentifera Farm 9
MicG Dentifera Farm 7
MicG Dentifera Farm 6
MicG Dentifera Farm 5
MicG Dentifera Farm 4
MicG Dentifera Walsh 092021 9
MicG Dentifera Walsh 092021 7
MicG Dentifera Farm 8
MicG Dentifera Walsh 092021 6
MicG Dentifera Walsh 092021 3
MicG Dentifera Walsh 092021 2
Ordospora pajunii JACCJH010000022.1
Microsporidium sp. MIC3 FJ794855.1
Ordospora colligata AF394529.1
Ordospora colligata XR 001377306.1 + 307.1
0.020
C)
MicG Dentifera Walsh
Ordospora pajunii FI-F-10
Ordospora colligata FI-SK-17-1
Ordospora colligata NO-V-7
Ordospora colligata GB-EP-1
Ordospora colligata OC4
Encephalitozoon hellem ATCC50504
Encephalitozoon romaleae SJ-2008
Encephalitozoon intestinalis ATCC50506
Encephalitozoon cuniculi GB-M1
Nosema ceranae BRL
Nosema apis BRL01
Nosema granulosis Ou3-Ou53
Nosema bombycis CQ1
Enterocytozoon hepatopenaei CIBAehp1
Enterospora canceri GB1
Enterocytozoon bieneusi H348
Hepatospora eriocheir GB1
Vittaforma corneae ATCC50505
Tubulinosema ratisbonensis Franzen
Anncaliia algerae PRA339
Antonospora locustae CLX
Hamiltosporidium tvaerminnensis FI-OER-3-3
Hamiltosporidium magnivora BE-OM-2
Thelohania contejeani T1
Edhazardia aedis USNM41457
Dictyocoela muelleri Ou54
Dictyocoela roeselum Ou19
Spraguea lophii Celtic Deep
Cucumispora dikerogammari Dv6
Pseudoloma neurophilia MK1
Trachipleistophora hominis
Vavraia culicis floridensis
Nematocida parisii ERTm1
Nematocida ironsii ERTm5
Nematocida ausubeli ERTm6
Nematocida displodere JUm2807
Metchnikovella incurvata LNA5
Amphiamblys sp. WSBS2006
0.5

369
370

Figure 1. Phylogenetic analyses suggest a close affinity of MicG and the recently described *O. pajunii*. A) A maximum likelihood phylogenetic tree of partial SSU ribosomal RNA sequences reveals no variation within MicG, and high similarity to *O. pajunii*. The sequence labeled “Microsporidium sp. MicG MH635259.1" was previously sequenced as part of the Rogalski et al. (6) study. B) ITS sequences of MicG were also identical and very similar to that of *O. pajunii*. In A&B, the branch support is based on 1000x bootstrap replicates, and the scale corresponds to the branch length and represents the number of substitutions per site. C) A maximum likelihood phylogenetic tree of 332 genes from the microsporidia_odb10 database also supports very high similarity between MicG and *O. pajunii*; branch support is based on 100x bootstrap replicates. MicG and *O. pajunii* are indicated with orange and purple rectangles, respectively.

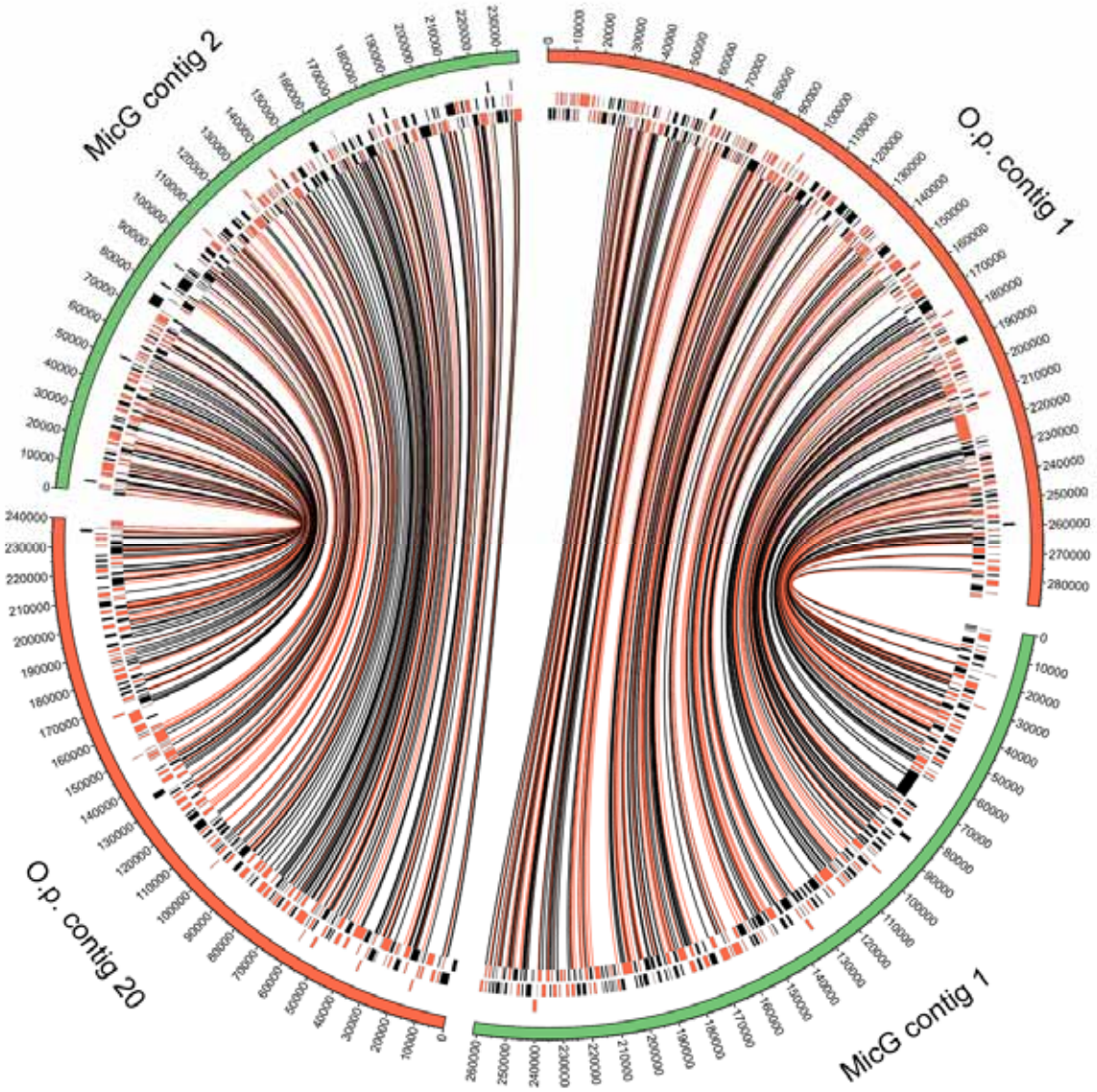

Figure 2. Comparison of two largest contigs of MicG with homologous contigs of *O. pajunii* shows conserved gene order. The outer band shows the lengths of chromosomes, and the inner rings are the locations of the genes, arbitrarily split into three lines to prevent overlap for clarity (black markers are on + strand and orange markers on - strand). Links connect SNPs identified following alignment and are indicated as amino acid changing (orange) or silent (black). Plot generated using Circos (37).

Microscopy

We observed the first symptoms of infection about 7-10 days after exposure. Infection is visible as white globular structures embedded within the host's gut epithelium (Figure 2A, B). At first, only several clusters of the parasite spores are visible. Spores initially occupy the central part of the host's cell (Figure 2G), but as they grow and divide, the vacuole containing them starts

397 expanding and growing towards the inside of the host's gut (Figure 2H). At the late stage of
398 cluster development, the cluster is visible as a bubble-shaped sac (Figure 2C, D) waved by the
399 peristalsis of the host's gut. The vacuole eventually bursts, releasing the spores into the gut
400 lumen (Figure 2C, I). The spores are then shed into the environment, although it is possible that
401 some reinfect the same host prior to release into the environment. Interestingly, electron
402 microscopy revealed that the microvilli are absent from the epithelial cells in these later stages
403 of cluster development, when the cluster has moved towards (or into) the gut lumen (Figure 2F,
404 H, I).
405
406 Initial infections most frequently occur in the upper part of the midgut and diverticula. Over time,
407 the number of clusters and general coverage of the gut by the parasite increases, resulting in
408 tens to hundreds of clusters spread across the gut, frequently merging into an indistinguishable
409 mass (Figure 2A, B). The spores are about 3.03 µm long (range: 2.57-3.71, n=100) and 1.66 µm
410 wide (range: 1.45-1.96, n=100), initially oval (Figure 2J, K) and pyriform when mature (Figure
411 2D, E). The size of MicG spores overlaps with *O. colligata* and the *O. pajunii* isolate described
412 by de Albuquerque et al. (12); however, unlike those, MicG does not form chains when extruded
413 from the host (Figure 2E).

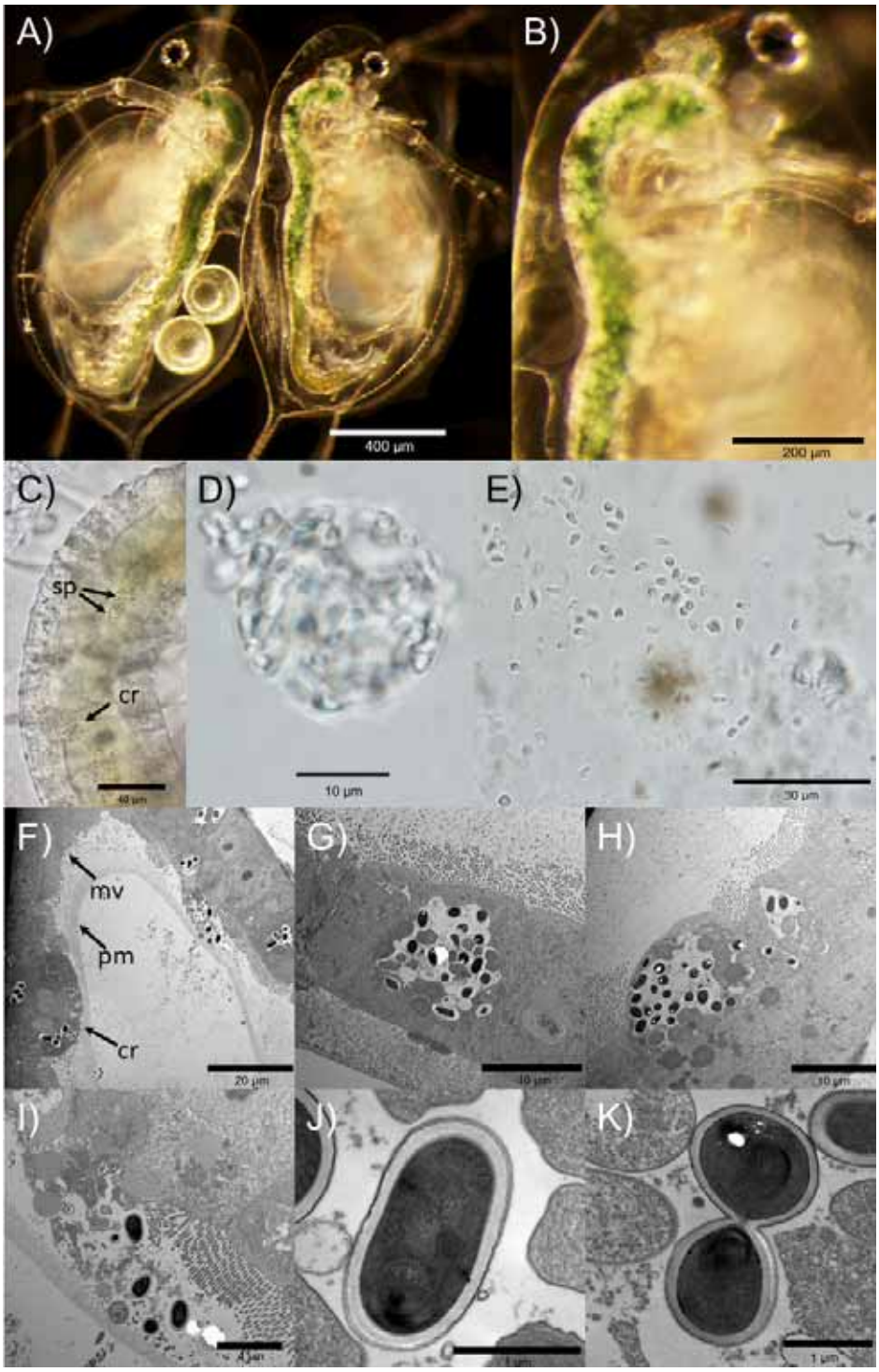

Figure 2. A) *D. dentifera* infected with *O. pajunii* (on the right) vs. uninfected *Daphnia* (on the left), B) the same infected *Daphnia* as in 'A', at higher magnification, C) upper part of midgut of an infected *Daphnia*, with a mature spore cluster (cr) and visible spores coming from a burst cluster (sp), D) a cluster of *O. pajunii* spores extracted from the gut, E) free floating spores extruded from the gut - after extracting a host's gut, the clusters rapidly burst and release the

421 spores, F) cross section of an infected host's gut with visible microvilli (mv), peritrophic
422 membrane (pm) and a maturing spore cluster (cr), G) a spore cluster in a central part of the
423 epithelial cell, H) a more advanced spore cluster growing towards the inside of the gut lumen, I)
424 spores released from the host's cell after a cluster burst, J) a single cell of *O. pajunii*, and K) a
425 late stage of cell division.
426
427
428
429 *Life table measures of parasite virulence*
430 Infection prevalence varied across genotypes from 0-100% infected individuals (Figure 3A).
431 Early exposure to parasite spores tended to result in higher infection success among the
432 susceptible clones, although in the case of clone BD08 higher prevalence was observed in the
433 late exposure treatment. Additionally, we observed consistent variation in the morphology of
434 infection across genotypes (Figure 3B). Infection in the S clone manifests as densely filled
435 globules with defined edges; in BD08, infection frequently manifests with a grainy appearance
436 where the clusters are much smaller and more dispersed; finally, in DW22, infection manifests
437 as an amorphous cloudy patch in the gut.
438
439 Total lifetime fecundity varied depending on parasite treatment and clone (interaction:
440 $F_{6,108}$=5.945, P<0.0001). More specifically, the S genotype produced fewer offspring than the
441 controls if they had been exposed early in life (i.e., the MicG48 treatment; T_{108}=4.908,P=0.0002)
442 and marginally fewer if they were exposed later (i.e., the MicG120 treatment; T_{108}=3.297,
443 P=0.076, Figure 3C). In addition, the DW29 genotype differed between parasite treatments, with
444 early exposure animals (i.e., the MicG48 treatment) producing fewer offspring compared to later
445 exposure (i.e., MicG120, T_{108}=4.082, p=0.006, Figure 3C). Host body size did not differ
446 depending on parasite treatment ($F_{2,69}$= 0.1482, P=0.8626). Host time to death differed due to
447 parasite treatment, but only for the S genotype; the lifespan of this genotype was significantly
448 shorter in the early parasite exposure compared to the no parasite treatment (hazard
449 ratio=4.577, 95%CI=1.616-12.964, P=0.0042, Figure 3D).
450
451

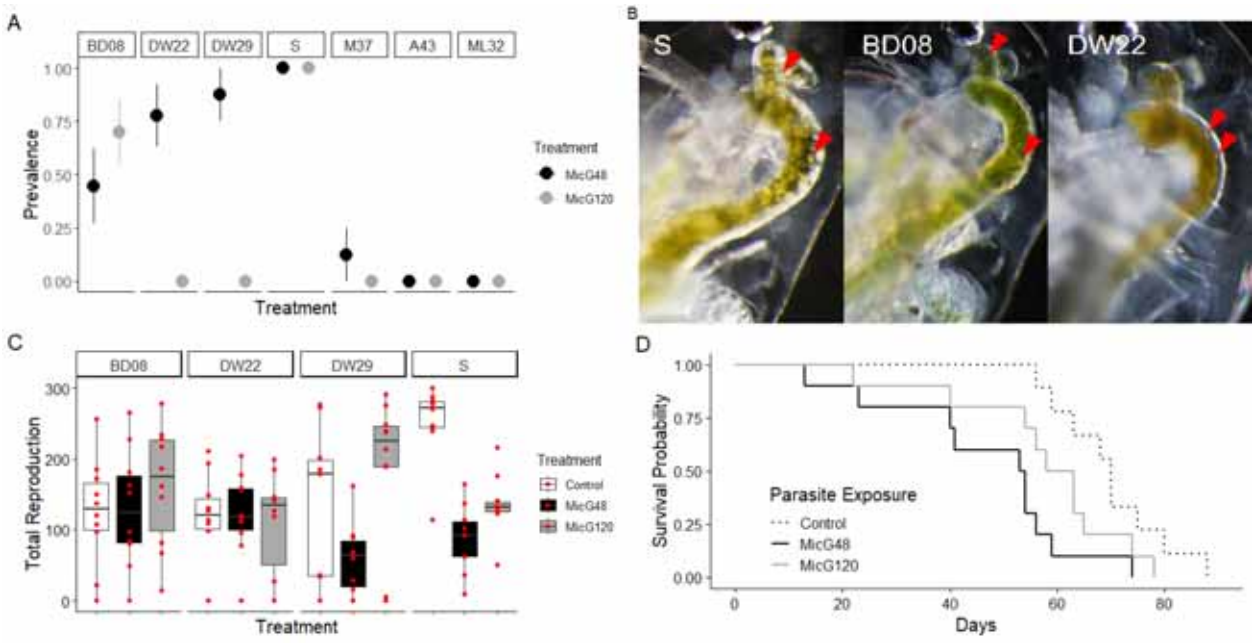

Figure 3. Genotypes differed in their likelihood of becoming infected, in the morphology of infection in the gut, and in the impact of infection. A) Varying proportion of animals of each clone (clone name indicated on top) displaying visible infection. The point and error bar represents the binomial mean and standard error. B) Morphology of infection with MicG in three of the susceptible clones: S, BD08, DW22. The red arrows indicate examples of MicG clusters. C) The parasite impacts lifetime total reproduction (that is, the total number of offspring produced across the experiment) in genotypes differently. The horizontal line represents a median, the boxes show first and third quartile and the whiskers represent the 1.5*IQR from the top and bottom. Raw data are overlaid in red. D) Time to event analysis for mortality indicated that only the lifespan of the S genotype was impacted by MicG. S genotype lifespan was significantly shortened with early exposure (solid black line) compared to no parasite exposure (dashed line).

Parasite prevalence in natural populations

Two of the four lakes, North and Pickerel, had sustained outbreaks of MicG (Figure 4). North Lake already had ~20% of *D. dentifera* adults infected at the beginning of the sampling period (in late July and early August). In North Lake, infection prevalence reached its maximum in mid-September (48% of the total *D. dentifera* population, 77% of adult females); in Pickerel, infection prevalence reached its maximum in the first half of October (57% of the total *D. dentifera* population, 70.5% of adult females). Infections were much lower in the other two lakes, except for a spike in infections in Sullivan near the end of the sampling period (in November); the population size remained high through this time, so this increase is not an artifact of low sample sizes (Figure S3).

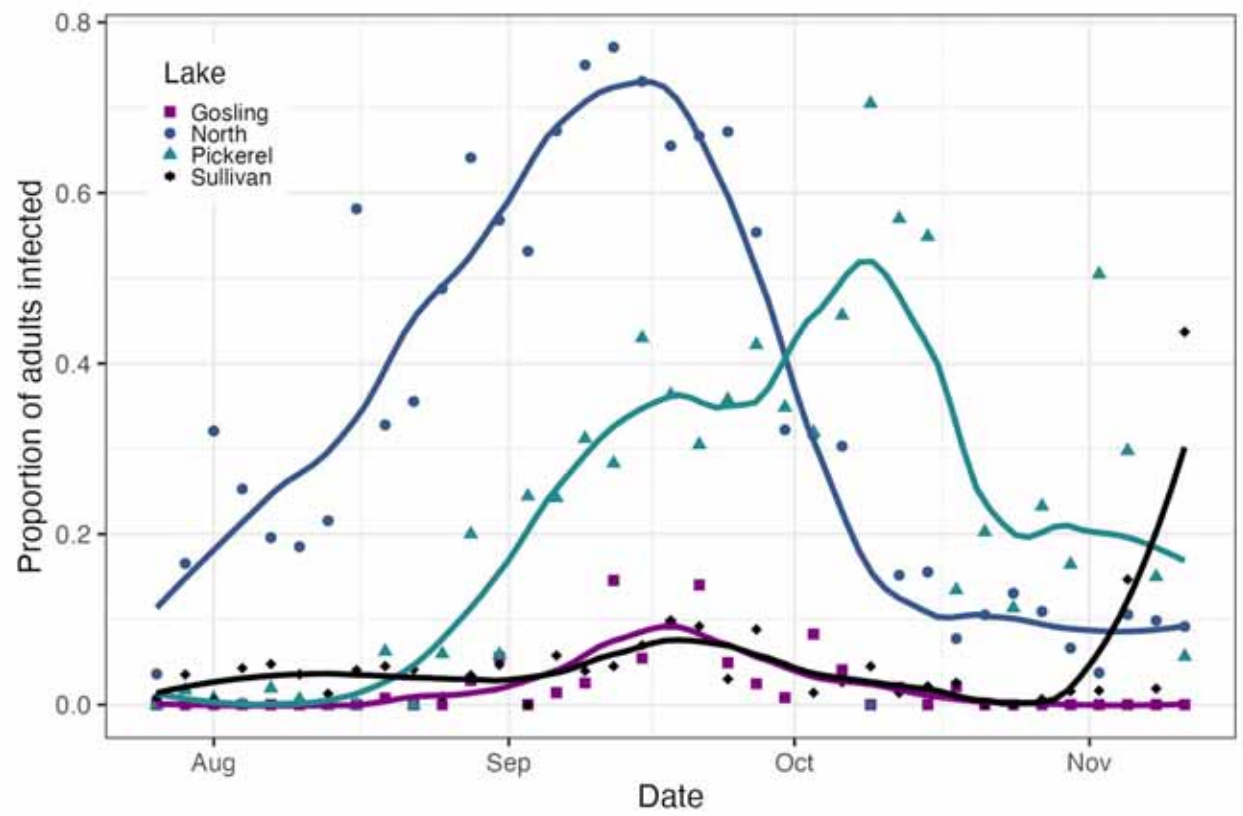

Figure 4. The proportion of *D. dentifera* adults that were infected with MicG varied over time and across lakes. Data come from four lakes (Gosling, North, Pickerel, and Sullivan) in Southeast Michigan, USA, that were sampled every three days in 2016.

Host range

We observed MicG infections in *Ceriodaphnia dubia*, *Daphnia ambigua*, *D. dentifera*, *D. dubia*, *D. mendotae*, *D. parvula*, *D. pulicaria* and *D. retrocurva* – that is, all of the *Daphnia* and *Ceriodaphnia* species in our study lakes. In addition, in our laboratory infection assay, MicG infected two out of the five *D. longispina* clones. Similar to *D. dentifera*, exposed *D. longispina* clones varied in their susceptibility to MicG (spanning 0% to 90%, Table S3).

Discussion

Prior ecological studies on this microsporidian have shown a clear impact on its host and on other symbionts competing for the same host (6, 9), as well as shifts along a mutualism-parasitism continuum; this all suggests promise as an interesting study system, especially since the host is already a model organism (10, 11, 38). In the present study, we characterized the phylogeny, morphology, virulence, ecology, and host range of this symbiont, with a goal of facilitating future work. Our phylogenetic analyses indicate very high similarity between MicG and *Ordospora pajunii,* a microsporidian recently described from *Daphnia longispina* in Europe (12). The spore morphology of both microsporidians is alike and both infections have similar presentation in the host's gut, overgrowing the epithelium and being successively shed and excreted with feces. We found MicG infections to be capable of reducing reproduction and lifespan of the most susceptible hosts, but the susceptibility to infection can strongly vary

504 between host genotypes. The host range of MicG spans across multiple *Daphnia* species; we
505 also found it was also able to infect members of a second genus, *Ceriodaphnia* sp.. Moreover,
506 MicG was capable of infecting *D. longispina*, the host from which *O. pajunii* was described (12),
507 which is not present in North America. Overall, our data indicates that MicG and *O. pajunii* are
508 the same species, hence the microsporidium previously called "MicG" (6, 9, 35) should be
509 considered *Ordospora pajunii*.
510
511 The high similarity across the entire genomes of MicG and *O. pajunii*, as well as complete
512 concordance of sequences at the SSU region and minimal difference at the ITS locus between
513 MicG and *O. pajunii* from Europe, lead us to conclude that they are the same species.
514 Nonetheless, we found some differences between North American and European *O. pajunii*. We
515 identified genetic divergence in some of the coding regions – most notably a 30 bp indel in the
516 *chitin synthase* gene. The sequence of the MicG *chitin synthase* gene in this region is almost
517 identical to that of *O. colligata* (Figure S2), suggesting a deletion in European *O. pajunii*. We
518 also identified multiple missense and nonsense mutations in other genes, when comparing the
519 genomes of MicG with *O. pajunii*. There are also some phenotypic differences, including that
520 spores of both *O. colligata* and *O. pajunii* isolated from Europe form chains (12), whereas MicG
521 spores do not; this is particularly notable, as the formation of chains has been proposed as
522 diagnostic for the genus *Ordospora* (12). In addition, *O. pajunii* infections are much less
523 pronounced in the hepatic caeca of the host than in the main midgut epithelium (12), and *O.*
524 *colligata* frequently develops intensively in the caeca (12); in contrast, MicG infects the caeca as
525 frequently as the midgut epithelium, and the intensity of the infection can vary temporally
526 between the two parts of the host's gut. Last but not least, MicG seems to have a much broader
527 range of susceptible host species than initially found for the described isolate of *O. pajunii* and
528 *O. colligata* (12).
529
530 The number of host species that we observed infected (all nine of the host species studied,
531 including those that were rare, such as *D. mendotae*) is also interesting because most
532 microsporidia are highly host species specific (39), with only 2.2% being able to infect >4 host
533 species (40). Prior studies on the genus *Ordospora* also suggested high specificity with regards
534 to host species: *O. colligata* is found only in *Daphnia magna* (41), and the initial study describing
535 *O. pajunii* found it was easily transmittable between clones of *D. longispina*, but not infectious to
536 the two genotypes of *Daphnia magna* that were tested in lab assays (12). We confirmed MicG
537 infections in 8 host species from two different genera in nature, and we found that it is capable
538 of infecting allopatric *D. longispina* despite substantial geographic isolation. The broad host
539 range found for MicG is atypical but not unknown for microsporidia. For example, members of
540 the genus *Encephalitozoon* are able to infect a broad spectrum of mammalian and avian hosts
541 (42). *Encepahliozoon* spp. and *Ordospora* spp. form a common clade, indicating high genetic
542 relatedness of the two genera; it is possible that their mechanisms of infection and interaction
543 with host immune defense are similar. The specific determinants of infection success and host
544 specificity in microsporidia are still being discovered, but molecular mechanisms and specifically
545 genetic matching seem to be the most obvious target of further investigation (39).
546

547 Broadly speaking, studies of molecular patterns of infection have provided substantial evidence
548 for the importance of genetic compatibility between host and parasite (43). More specifically,
549 gene-by-gene interactions have been found to determine successful infection of *Daphnia* by its
550 parasites. For example, infections by two microsporidia, *O. colligata* and *Hamiltosporidium*
551 *tvaerminnensis*, were found to be largely determined by very few host resistance genes, with
552 some of the genes being common for infections with both parasites (44, 45). Similarly, infection
553 of a bacterial parasite of *Daphnia*, *Pasteuria ramosa*, is determined by several genes regulating
554 the host's resistance (46, 47) and few genes determining the parasite's infectivity (44, 48). *P.*
555 *ramosa*, similarly to MicG, is found to infect multiple *Daphnia* species (49, 50). The likelihood of
556 multiple host species being susceptible to the same parasite species increases with increasing
557 relatedness of the hosts (51, 52). As pathogens tend to consistently interact with the same
558 genes across the host species (53), it is likely that high similarity of immunity genes/proteins
559 among related host species enables a pathogen to infect multiple species. In the case of *P.*
560 *ramosa*, not only the genes but also the alleles that determine whether a spore can attack a
561 particular host individual are maintained across the *Daphnia* genus (54, 55). Hence the
562 bacterium is infectious to multiple *Daphnia* species, including a single strain being capable of
563 infections across host species, albeit rarely (54, 55). Given the substantial variation in
564 susceptibility to MicG among the tested *D. dentifera* (from 0 to 100% infection prevalence) and
565 *D. longispina* (0 to 90%) clones, and the broad range of host species of this microsporidium, it
566 seems plausible that alleles involved in susceptibility to MicG could be conserved across host
567 species, like in the case of *P. ramosa*. Future studies that explore the degree of host-parasite
568 genotype specificity (as done, for example, in Carius et al. (56)), as well as the structuring of the
569 genetic variation of the parasite by host species and geography (as done by Shaw et al. (57))
570 would help uncover the factors determining the likelihood of infection within and across host
571 species.
572
573 Genetic matching between host and parasite is just one of many factors determining infection
574 success in microsporidia (39); factors such as developmental stage and feeding behavior of the
575 host also seem relevant to the *Daphnia* - MicG interaction. For example, some microsporidia are
576 more infectious to their host in its early larval stages (58) whereas others are more successful
577 infecting older life stages (59). Our results indicate that MicG is generally more infectious to
578 younger *Daphnia*, although this effect seems to be clone-specific. The sister-microsporidian *O.*
579 *colligata* was also found to be more successful infecting younger *D. magna* than older ones
580 (60). A similar pattern of higher susceptibility of a younger host was found in *D. magna* exposed
581 to the bacterium *P. ramosa*, and the proposed explanation was that immune defense
582 mechanisms are less efficient in younger instars of *Daphnia* (61). In contrast, older *D. dentifera*
583 are more susceptible to the fungus *Metschnikowia bicuspidata*, possibly due to the higher
584 feeding rates of older (and, therefore, larger) hosts (62). Because *Daphnia* encounter parasites
585 while foraging for phytoplankton, feeding rates determine the contact rate of the host with many
586 parasites, including bacteria, fungi and microsporidia (60, 62–64). Even in cases where younger
587 hosts are more susceptible to parasites, variation in feeding rates might still play an important
588 role in determining patterns of infection. As higher contact rate with infectious spores can
589 increase the likelihood of becoming infected (62, 63, 65), host genotypes with higher feeding
590 rates (63, 66) can be more susceptible to parasitic infections than the slow feeders (63). Hence,

591 variation among genotypes in feeding behavior could be another factor driving the variation in
592 susceptibility to MicG observed among our *D. dentifera* clones.
593
594 While the infectivity of MicG largely varied between tested clones, the virulence was rather
595 uniform. We found a significant reduction in lifespan and reproduction of the host in only one
596 genotype; the other *Daphnia* genotypes seemed largely unaffected by MicG. Low virulence
597 could be one of the critical traits enabling MicG to generate a net positive outcome to its host
598 when a more virulent parasite is in the environment (as found by Rogalski et al. (6)) — low basal
599 virulence would require much less positive impact to tip the scale from parasitism to mutualism.
600 However, a different study on this system found a novel phenomenon of transgenerational
601 virulence, where the offspring of hosts exposed to MicG suffered reduced fitness; this indicates
602 that the virulence of MicG might primarily manifest in the progeny of exposed hosts (67).
603 Therefore, we recommend interpreting the findings of low within-generation virulence cautiously,
604 and at the same time recommend considering the impact of any symbiont on its host not only
605 based on a within-generation snapshot, but across generations as well. The clone that
606 expressed the strongest transgenerational virulence effect, the S clone (referred to as “S” also
607 in (67)), was also the most susceptible to MicG and suffered most from virulent effects of
608 infection in this study. The particularly strong effect on that host may be due to unintended
609 selection imposed as a result of our culturing – we maintain our lab *O. pajunii* culture in the S
610 clone; therefore, the parasite isolate that we used in this study is likely strongly adapted to
611 exploit this clone. While the high virulence in this host genotype might reflect selection in the
612 lab, that does not mean that such virulence is not also occurring in nature — it is likely that each
613 outbreak is composed of multiple MicG strains varying in their infectivity and virulence to
614 different clones, potentially leading to selection favoring the parasite strains best adapted to
615 exploit the most abundant hosts (48, 68). Future studies that explore variation in virulence of
616 different *O. pajunii* isolates, as well as the potential for rapid adaptation on the part of the
617 parasite, would help us better understand the ecological and evolutionary dynamics of this
618 system. Moreover, it will help determine whether some of the variation in fitness impacts of
619 infection observed in the field (6) result from variation in the virulence of the parasite due to host
620 and/or parasite genetic variation.
621
622 The virulence of MicG might be a result of its direct impact to the host's gut. The microsporidium
623 frequently covers most of the midgut area in heavily infected hosts. An earlier study found that
624 *O. pajunii* reduces the penetrability of the guts of infected hosts to other parasites (6), and our
625 study found changes in the morphology of the gut. Most notably, microvilli were not visible next
626 to epithelial cells with more developed infections, when the cluster had moved towards or into
627 the gut lumen. These changes are intriguing, as they suggest that *O. pajunii* infections should
628 strongly alter host interactions with other parasites and resources — both the reduced
629 penetrability and the loss of microvilli should impair resource assimilation. This would be further
630 accentuated if *Daphnia* infected with *O. pajunii* lower their feeding rate; illness mediated
631 anorexia is common in hosts (69), including *Daphnia* infected with other parasites (63, 70).
632 Diminished feeding rate would reduce the contact rate of the host with other parasites (thus
633 reducing the likelihood of infection (62–64, 71)) and host nutrition (which decreases host fitness
634 (63, 64)), making the beneficial impact of MicG contingent upon the presence of other parasites

and food resources. Together, these impacts on gut morphology – as well as potential impacts on feeding rate – have the potential to impact not only host fitness, but also ecosystem-level processes such as primary productivity and nutrient cycling. Given that *Daphnia* are the dominant grazers in many lakes, and the very high prevalence of infection in some populations (Figure 4), we propose that *O. pajunii* outbreaks might have important ecosystem-level consequences.

Our genetic analyses of the microsporidian symbiont of *Daphnia* formerly referred to as "MicG" (6, 9, 35) revealed that it belongs to *Ordospora pajunii* (12). It is found in North American lakes as well as coastal ponds in Finland, which suggests a very broad geographical distribution. It also has an intriguingly broad host distribution, infecting a wide range of *Daphnia* species as well as *Ceriodaphnia*. Our study found *O. pajunii* has modest effects on survival and reproduction within a generation, and prior work suggested context dependence of the fitness impact on hosts (6); moreover, other evidence suggests virulent effects might primarily occur in the next generation (67). Some of the virulence might relate to the destructive effects of the microsporidian on host gut morphology, with the potential for this to substantially alter interactions of this dominant herbivore with its resources. Altogether, this *Daphnia*-microsporidian system seems highly promising for future studies aimed at uncovering the ecology and evolution of host-parasite interactions in the wild.

Acknowledgements

We thank Justyna Wolinska for the *D. longispina* clones. We also thank the members of the Duffy Lab who helped collect and process the field samples during the host range portion of this study – Rebecca Bilich, Siobhan Calhoun, Kate McLean, Kira Monell, Kristel Sánchez, Teresa Sauer, and Syuan-Jyun Sun. This work was supported by NSF grants DEB-1305836 and DEB-1748729 and by the Gordon and Betty Moore Foundation (GBMF9202; DOI: https://doi.org/10.37807/GBMF9202). The work (proposal 10.46936/10.25585/60001004) conducted by the U.S. Department of Energy Joint Genome Institute (https://ror.org/04xm1d337), a DOE Office of Science User Facility, is supported by the Office of Science of the U.S. Department of Energy under Contract No. DE-AC02-05CH11231. This project was funded in part by the National Science Foundation grant DEB-1929738 to TYJ. TYJ is a fellow of the Canadian Institute for Advanced Research program Fungal Kingdom: Threats & Opportunities. KS was supported by JSPS Overseas Research Fellowships (No. 201960485).

References

1. Johnson NC, Graham J-H, Smith FA. 1997. Functioning of mycorrhizal associations along the mutualism–parasitism continuum*. *New Phytologist* 135:575–585.
2. Drew GC, Stevens EJ, King KC. 2021. Microbial evolution and transitions along the parasite–mutualist continuum. *Nature Reviews Microbiology* 19:623–638.

677 3. Canestrari D, Bolopo D, Turlings TCJ, Röder G, Marcos JM, Baglione V. 2014. From
678 parasitism to mutualism: Unexpected interactions between a cuckoo and its host. *Science*
679 343:1350–1352.
680 4. Baker DM, Freeman CJ, Wong JCY, Fogel ML, Knowlton N. 2018. Climate change
681 promotes parasitism in a coral symbiosis. *The ISME Journal* 12:921–930.
682 5. Zhang H, Xie J, Fu Y, Cheng J, Qu Z, Zhao Z, Cheng S, Chen T, Li B, Wang Q, Liu X, Tian
683 B, Collinge DB, Jiang D. 2020. A 2-kb mycovirus converts a pathogenic fungus into a
684 beneficial endophyte for Brassica protection and yield enhancement. *Molecular Plant*
685 13:1420–1433.
686 6. Rogalski MA, Merrill TS, Gowler C, Caceres C, Duffy M. 2021. Context-dependent host-
687 symbiont interactions: shifts along the parasitism–mutualism continuum. *The American*
688 *Naturalist* 198:563–575.
689 7. Keeling Patrick J., Slamovits Claudio H. 2004. Simplicity and complexity of microsporidian
690 genomes. *Eukaryotic Cell* 3:1363–1369.
691 8. Dean P, Hirt RP, Embley TM. 2016. Microsporidia: Why make nucleotides if you can steal
692 them? *PLOS Pathogens* 12:e1005870.
693 9. Westphal GH, Stewart Merrill TE. 2022. Partitioning variance in immune traits in a
694 zooplankton host—Fungal parasite system. *Ecology and Evolution* 12:e9640.
695 10. Seda J, Petrusek A. 2011. Daphnia as a model organism in limnology and aquatic biology:
696 introductory remarks. *Journal of Limnology* 70:337–344.
697 11. Miner BE, De Meester L, Pfrender ME, Lampert W, Hairston Jr NG. 2012. Linking genes to
698 communities and ecosystems: Daphnia as an ecogenomic model. *Proceedings of the*
699 *Royal Society B* 279:1873–1882.
700 12. de Albuquerque NRM, Haag KL, Fields PD, Cabalzar A, Ben-Ami F, Pombert J-F, Ebert D.
701 2022. A new microsporidian parasite, Ordospora pajunii sp. nov (Ordosporidae), of
702 Daphnia longispina highlights the value of genomic data for delineating species

boundaries. Journal of Eukaryotic Microbiology 69:e12902.

13. Tessier AJ, Woodruff P. 2002. CRYPTIC TROPHIC CASCADE ALONG A GRADIENT OF LAKE SIZE. Ecology 83:1263–1270.

14. Duffy MA, Caceres CE, Hall SR, Tessier AJ, Ives AR. 2010. Temporal, spatial, and between-host comparisons of patterns of parasitism in lake zooplankton. Ecology 3322–3331.

15. Duffy Meghan A., James Timothy Y., Longworth Alan, Drake H. L. 2015. Ecology, Virulence, and Phylogeny of Blastulidium paedophthorum, a Widespread Brood Parasite of Daphnia spp. Applied and Environmental Microbiology 81:5486–5496.

16. Keeling PJ. 2014. Phylogenetic Place of Microsporidia in the Tree of Eukaryotes, p. 195–202. *In* Microsporidia.

17. James TY, Stajich JE, Hittinger CT, Rokas A. 2020. Toward a Fully Resolved Fungal Tree of Life. Annu Rev Microbiol 74:291–313.

18. Schoch CL, Seifert KA, Huhndorf S, Robert V, Spouge JL, Levesque CA, Chen W, null null, null null, Bolchacova E, Voigt K, Crous PW, Miller AN, Wingfield MJ, Aime MC, An K-D, Bai F-Y, Barreto RW, Begerow D, Bergeron M-J, Blackwell M, Boekhout T, Bogale M, Boonyuen N, Burgaz AR, Buyck B, Cai L, Cai Q, Cardinali G, Chaverri P, Coppins BJ, Crespo A, Cubas P, Cummings C, Damm U, de Beer ZW, de Hoog GS, Del-Prado R, Dentinger B, Diéguez-Uribeondo J, Divakar PK, Douglas B, Dueñas M, Duong TA, Eberhardt U, Edwards JE, Elshahed MS, Fliegerova K, Furtado M, García MA, Ge Z-W, Griffith GW, Griffiths K, Groenewald JZ, Groenewald M, Grube M, Gryzenhout M, Guo L-D, Hagen F, Hambleton S, Hamelin RC, Hansen K, Harrold P, Heller G, Herrera C, Hirayama K, Hirooka Y, Ho H-M, Hoffmann K, Hofstetter V, Högnabba F, Hollingsworth PM, Hong S-B, Hosaka K, Houbraken J, Hughes K, Huhtinen S, Hyde KD, James T, Johnson EM, Johnson JE, Johnston PR, Jones EBG, Kelly LJ, Kirk PM, Knapp DG, Kõljalg U, Kovács GM, Kurtzman CP, Landvik S, Leavitt SD, Liggenstoffer AS, Liimatainen K, Lombard L,

729 Luangsa-ard JJ, Lumbsch HT, Maganti H, Maharachchikumbura SSN, Martin MP, May
730 TW, McTaggart AR, Methven AS, Meyer W, Moncalvo J-M, Mongkolsamrit S, Nagy LG,
731 Nilsson RH, Niskanen T, Nyilasi I, Okada G, Okane I, Olariaga I, Otte J, Papp T, Park D,
732 Petkovits T, Pino-Bodas R, Quaedvlieg W, Raja HA, Redecker D, Rintoul TL, Ruibal C,
733 Sarmiento-Ramírez JM, Schmitt I, Schüßler A, Shearer C, Sotome K, Stefani FOP,
734 Stenroos S, Stielow B, Stockinger H, Suetrong S, Suh S-O, Sung G-H, Suzuki M, Tanaka
735 K, Tedersoo L, Telleria MT, Tretter E, Untereiner WA, Urbina H, Vágvölgyi C, Vialle A, Vu
736 TD, Walther G, Wang Q-M, Wang Y, Weir BS, Weiß M, White MM, Xu J, Yahr R, Yang ZL,
737 Yurkov A, Zamora J-C, Zhang N, Zhuang W-Y, Schindel D. 2012. Nuclear ribosomal
738 internal transcribed spacer (ITS) region as a universal DNA barcode marker for Fungi.
739 *Proceedings of the National Academy of Sciences* 109:6241–6246.
740 19. Davis WJ, Amses KR, Benny GL, Carter-House D, Chang Y, Grigoriev I, Smith ME,
741 Spatafora JW, Stajich JE, James TY. 2019. Genome-scale phylogenetics reveals a
742 monophyletic Zoopagales (Zoopagomycota, Fungi). *Molecular Phylogenetics and*
743 *Evolution* 133:152–163.
744 20. Bankevich A, Nurk S, Antipov D, Gurevich AA, Dvorkin M, Kulikov AS, Lesin VM,
745 Nikolenko SI, Pham S, Prjibelski AD, Pyshkin AV, Sirotkin AV, Vyahhi N, Tesler G,
746 Alekseyev MA, Pevzner PA. 2012. SPAdes: A new genome assembly algorithm and its
747 applications to single-cell sequencing. *Journal of Computational Biology* 19:455–477.
748 21. Grigoriev IV, Nikitin R, Haridas S, Kuo A, Ohm R, Otillar R, Riley R, Salamov A, Zhao X,
749 Korzeniewski F, Smirnova T, Nordberg H, Dubchak I, Shabalov I. 2014. MycoCosm portal:
750 gearing up for 1000 fungal genomes. *Nucleic Acids Research* 42:D699–D704.
751 22. Manni M, Berkeley MR, Seppey M, Simão FA, Zdobnov EM. 2021. BUSCO update: Novel
752 and streamlined workflows along with broader and deeper phylogenetic coverage for
753 scoring of eukaryotic, prokaryotic, and viral genomes. *Molecular Biology and Evolution*
754 38:4647–4654.

755 23. McGowan J, O'Hanlon R, Owens RA, Fitzpatrick DA. 2020. Comparative genomic and
756 proteomic analyses of three widespread Phytophthora species: Phytophthora
757 chlamydospora, Phytophthora gonapodyides and Phytophthora pseudosyringae.
758 *Microorganisms* 8.
759 24. Capella-Gutiérrez S, Silla-Martínez JM, Gabaldón T. 2009. trimAl: a tool for automated
760 alignment trimming in large-scale phylogenetic analyses. *Bioinformatics* 25:1972–1973.
761 25. Minh BQ, Schmidt HA, Chernomor O, Schrempf D, Woodhams MD, von Haeseler A,
762 Lanfear R. 2020. IQ-TREE 2: New models and efficient methods for phylogenetic inference
763 in the genomic era. *Molecular Biology and Evolution* 37:1530–1534.
764 26. Wang H-C, Minh BQ, Susko E, Roger AJ. 2018. Modeling site heterogeneity with posterior
765 mean site frequency profiles accelerates accurate phylogenomic estimation. *Systematic*
766 *Biology* 67:216–235.
767 27. Chernomor O, von Haeseler A, Minh BQ. 2016. Terrace aware data structure for
768 phylogenomic inference from supermatrices. *Systematic Biology* 65:997–1008.
769 28. Lee I, Ouk Kim Y, Park S-C, Chun J. 2016. OrthoANI: An improved algorithm and software
770 for calculating average nucleotide identity. *International Journal of Systematic and*
771 *Evolutionary Microbiology* 66:1100–1103.
772 29. Treangen TJ, Ondov BD, Koren S, Phillippy AM. 2014. The Harvest suite for rapid core-
773 genome alignment and visualization of thousands of intraspecific microbial genomes.
774 *Genome Biology* 15:524.
775 30. Cingolani P, Platts A, Wang LL, Coon M, Nguyen T, Wang L, Land SJ, Lu X, Ruden DM.
776 2012. A program for annotating and predicting the effects of single nucleotide
777 polymorphisms, SnpEff. *Fly* 6:80–92.
778 31. Hyatt D, Chen G-L, LoCascio PF, Land ML, Larimer FW, Hauser LJ. 2010. Prodigal:
779 prokaryotic gene recognition and translation initiation site identification. *BMC*
780 *Bioinformatics* 11:119.

781 32. Emms DM, Kelly S. 2019. OrthoFinder: phylogenetic orthology inference for comparative
782 genomics. *Genome Biology* 20:238.
783 33. Duffy MA, Hall SR. 2008. Selective predation and rapid evolution can jointly dampen
784 effects of virulent parasites on Daphnia populations. *The American Naturalist* 171:499–
785 510.
786 34. Shaw CL, Hall SR, Overholt EP, Cáceres CE, Williamson CE, Duffy MA. 2020. Shedding
787 light on environmentally transmitted parasites: lighter conditions within lakes restrict
788 epidemic size. *Ecology* 101:e03168.
789 35. Gowler CD, Rogalski MA, Shaw CL, Hunsberger KK, Duffy MA. 2021. Density, parasitism,
790 and sexual reproduction are strongly correlated in lake Daphnia populations. *Ecology and*
791 *Evolution* 11:10446–10456.
792 36. Dia N, Lavie L, Faye N, Méténier G, Yeramian E, Duroure C, Toguebaye BS, Frutos R,
793 Niang MN, Vivarès CP, Ben Mamoun C, Cornillot E. 2016. Subtelomere organization in the
794 genome of the microsporidian Encephalitozoon cuniculi: patterns of repeated sequences
795 and physicochemical signatures. *BMC Genomics* 17:34.
796 37. Krzywinski M, Schein J, Birol İ, Connors J, Gascoyne R, Horsman D, Jones SJ, Marra MA.
797 2009. Circos: An information aesthetic for comparative genomics. *Genome Research*
798 19:1639–1645.
799 38. Ebert D. 2022. Daphnia as a versatile model system in ecology and evolution. *EvoDevo*
800 13:16.
801 39. Willis AR, Reinke AW. 2022. Factors That Determine Microsporidia Infection and Host
802 Specificity, p. 91–114. *In* Weiss, LM, Reinke, AW (eds.), Microsporidia: Current Advances
803 in Biology. Springer International Publishing, Cham.
804 40. Murareanu Brandon M., Sukhdeo Ronesh, Qu Rui, Jiang Jason, Reinke Aaron W. 2021.
805 Generation of a Microsporidia Species Attribute Database and Analysis of the Extensive
806 Ecological and Phenotypic Diversity of Microsporidia. *mBio* 12:e01490-21.

807 41. Larsson JIR, Ebert D, Vávra J. 1997. Ultrastructural study and description of Ordospora
808 colligata gen. et sp. nov. (microspora, ordosporidae fam. nov.), a new microsporidian
809 parasite of Daphnia magna (Crustacea, Cladocera). *European Journal of Protistology*
810 33:432–443.
811 42. Hinney B, Sak B, Joachim A, Kváč M. 2016. More than a rabbit's tale – Encephalitozoon
812 spp. in wild mammals and birds. *International Journal for Parasitology: Parasites and*
813 *Wildlife* 5:76–87.
814 43. Dybdahl MF, Jenkins CE, Nuismer SL. 2014. Identifying the molecular basis of host-
815 parasite coevolution: Merging models and mechanisms. *The American Naturalist* 184:1–
816 13.
817 44. Routtu J, Ebert D. 2015. Genetic architecture of resistance in Daphnia hosts against two
818 species of host-specific parasites. *Heredity* 114:241–248.
819 45. Keller D, Kirk D, Luijckx P. 2019. Four QTL underlie resistance to a microsporidian parasite
820 that may drive genome evolution in its Daphnia host. bioRxiv
821 https://doi.org/10.1101/847194
822 46. Ameline C, Voegtli F, Andras J, Dexter E, Engelstädter J, Ebert D. Genetic slippage after
823 sex maintains diversity for parasite resistance in a natural host population. *Science*
824 *Advances* 8:eabn0051.
825 47. Ameline C, Bourgeois Y, Vögtli F, Savola E, Andras J, Engelstädter J, Ebert D. 2021. A
826 two-locus system with strong epistasis underlies rapid parasite-mediated evolution of host
827 resistance. *Molecular Biology and Evolution* 38:1512–1528.
828 48. Andras JP, Fields PD, Du Pasquier L, Fredericksen M, Ebert D. 2020. Genome-wide
829 association analysis identifies a genetic basis of infectivity in a model bacterial pathogen.
830 *Molecular Biology and Evolution* 37:3439–3452.
831 49. Ebert D, Rainey P, Embley TM, Scholz D. 1996. Development, life cycle, ultrastructure and
832 phylogenetic position of Pasteuria ramosa Metchnikoff 1888: rediscovery of an obligate

833 endoparasite of Daphnia magna Straus. *Philosophical Transactions of the Royal Society of*
834 *London Series B: Biological Sciences* 351:1689–1701.
835 50. Shaw CL. 2019. Drivers of epidemic timing and size in a natural aquatic system. Doctoral
836 dissertation. University of Michigan, Michigan, USA.
837 https://deepblue.lib.umich.edu/handle/2027.42/151685.
838 51. Davies TJ, Pedersen AB. 2008. Phylogeny and geography predict pathogen community
839 similarity in wild primates and humans. *Proceedings of the Royal Society B: Biological*
840 *Sciences* 275:1695–1701.
841 52. Parker IM, Saunders M, Bontrager M, Weitz AP, Hendricks R, Magarey R, Suiter K, Gilbert
842 GS. 2015. Phylogenetic structure and host abundance drive disease pressure in
843 communities. *Nature* 520:542–544.
844 53. Shultz AJ, Sackton TB. 2019. Immune genes are hotspots of shared positive selection
845 across birds and mammals. *eLife* 8:e41815.
846 54. Luijckx P, Duneau D, Andras JP, Ebert D. 2014. Cross-species infection trials reveal
847 cryptic parasite varieties and a putative polymorphism shared among host species.
848 *Evolution* 68:577–586.
849 55. Duneau D, Luijckx P, Ben-Ami F, Laforsch C, Ebert D. 2011. Resolving the infection
850 process reveals striking differences in the contribution of environment, genetics and
851 phylogeny to host-parasite interactions. *BMC Biology* 9:11.
852 56. Carius HJ, Little TJ, Ebert D. 2001. Genetic variation in a host-parasite association:
853 potential for coevolution and frequency-dependent selection. *Evolution* 55:1136–1145.
854 57. Shaw CL, Bilich R, O'Brien B, Cáceres CE, Hall SR, James TY, Duffy MA. 2021.
855 Genotypic variation in an ecologically important parasite is associated with host species,
856 lake and spore size. *Parasitology* 148:1303–1312.
857 58. Blaser M, Schmid-Hempel P. 2005. Determinants of virulence for the parasite Nosema
858 whitei in its host Tribolium castaneum. *Journal of Invertebrate Pathology* 89:251–257.

59. Balla KM, Andersen EC, Kruglyak L, Troemel ER. 2015. A wild C. elegans strain has enhanced epithelial immunity to a natural microsporidian parasite. *PLOS Pathogens* 11:e1004583.

60. Kirk D, Luijckx P, Stanic A, Krkošek M. 2019. Predicting the thermal and allometric dependencies of disease transmission via the metabolic theory of ecology. *The American Naturalist* 193:661–676.

61. Izhar R, Ben-Ami F. 2015. Host age modulates parasite infectivity, virulence and reproduction. *Journal of Animal Ecology* 84:1018–1028.

62. Hall SR, Sivars-Becker L, Becker C, Duffy MA, Tessier AJ, Cáceres CE. 2007. Eating yourself sick: transmission of disease as a function of foraging ecology. *Ecology Letters* 10:207–218.

63. Auld SKJR, Raidma K. 2022. Host genetic variation in feeding rate mediates a fecundity cost of parasite resistance in a Daphnia-parasite system. bioRxiv https://doi.org/10.1101/2022.11.29.518345

64. Hall SR, Becker CR, Duffy MA, Cáceres CE. 2010. Variation in resource acquisition and use among host clones creates key epidemiological trade-offs. *The American Naturalist* 176:557–565.

65. Shocket MS, Vergara D, Sickbert AJ, Walsman JM, Strauss AT, Hite JL, Duffy MA, Cáceres CE, Hall SR. 2018. Parasite rearing and infection temperatures jointly influence disease transmission and shape seasonality of epidemics. *Ecology* 99:1975–1987.

66. Hite JL, Pfenning-Butterworth AC, Vetter RE, Cressler CE. 2020. A high-throughput method to quantify feeding rates in aquatic organisms: A case study with Daphnia. *Ecology and Evolution* 10:6239–6245.

67. McIntire KM, Dziuba MK, Haywood EB, Robertson ML, Vaandrager M, Baird E, Corcoran F, Cortez MH, Duffy MA. 2023. Transgenerational virulence: Maternal pathogen exposure reduces offspring fitness. bioRxiv https://doi.org/10.1101/2023.03.14.532659

68. Lively CM, Dybdahl MF. 2000. Parasite adaptation to locally common host genotypes. *Nature* 405:679–681.

69. Hite JL, Pfenning AC, Cressler CE. 2020. Starving the enemy? Feeding behavior shapes host-parasite interactions. *Trends in Ecology & Evolution* 35:68–80.

70. Penczykowski RM, Shocket MS, Ochs JH, Lemanski BCP, Sundar H, Duffy MA, Hall SR. 2022. Virulent disease epidemics can increase host density by depressing foraging of hosts. *The American Naturalist* 199:75–90.

71. Shocket MS, Strauss AT, Hite JL, Šljivar M, Civitello DJ, Duffy MA, Cáceres CE, Hall SR. 2018. Temperature drives epidemics in a zooplankton-fungus disease system: A trait-driven approach points to transmission via host foraging. *The American Naturalist* 191:435–451.

Supplemental Materials

Cultivating MicG in the laboratory

Establishing lab cultures

We established protocols for maintaining MicG in the *D. dentifera* clone S. These cultures were established in water from North Lake (Washtenaw County, Michigan, USA) that was filtered (with Pall AE glass microfiber filters) in order to remove algae, cyanobacteria, and debris from the water. To establish the MicG culture, we collected *D. dentifera* visibly infected with MicG from Walsh Lake (Washtenaw County, Michigan, USA). We grouped >10 individuals in a 1.5 mL centrifuge tube and ground them using a plastic pestle. We filled 24 centrifuge tubes (1.5 mL volume capacity), each with 1 mL of filtered lake water and introduced a single 0-2 day old *D. dentifera* (S clone) to each tube. Individuals were left in their tubes for 48 h to ingest the parasite spores. After two days we transferred each host individual to a separate 50 mL beaker, which we fed 20,000 cells/mL of *Ankistrodesmus falcatus* 3 times a week. We screened for infection after seven days, then checked at 3 day intervals. Each individual that was found to be infected was used to establish a separate 'farm'. New farms were started by moving a heavily infected *Daphnia* (i.e. *Daphnia* having tens to hundreds of microsporidian spore clusters) into a 300 mL beaker and adding 5 juveniles of the S clone. As the MicG farm grew, we increased its volume to 1 L.

Culture observations

Initially the number of infected *Daphnia* increases as the host population size increases. Due to the near-constant shedding of spores, host offspring quickly become infected, increasing the number of infected hosts. Soon after the host population size approaches the carrying capacity of the farm, the infection prevalence among adults frequently reaches 90-100%. In high prevalence farms, we tend to observe infection symptoms even in juveniles. We hypothesize that this is due to high spore concentrations in the environment. If prevalence is low, infections are infrequent in juveniles. The demography of the farm quickly shifts as the adults start producing non-viable embryos or stop producing embryos. Shortly thereafter, the host population collapses.

Molecular analyses

Accession numbers

SSU: OQ754180
ITS: OQ754181
Whole genome: In process

Figure S1. Alignment of proteins with the highest number of missense mutations (additional file).

Figure S2. Chitin synthase gene sequence alignment of *O. colligata*, MicG, *O. pajunii* and *E. cuniculi*.

Parasite prevalence in natural populations

The data on host range for daphnids in Southeastern Michigan came from a dataset that focused on 15 lakes in Livingston and Washtenaw Counties (Table S1). All of these lakes are stratified and include *D. dentifera* as a dominant member of the zooplankton. We also analyzed one sample from Lake Erie.

Table S1. Lakes sampled from 2016-2022 that provided information on host range (all 15 lakes), on the dynamics of infection (lakes in blue), and from which samples were collected for molecular analysis (lakes in red). Walsh Lake was the source of the MicG-infected individuals that were used to start the lab cultures.

Lake Name	Site	County	Latitude & Longitude	Max depth (m)
Appleton	Brighton	Livingston	42°30'37"N, 83°50'03"W	11.5
Bishop	Brighton	Livingston	42°30'04"N, 83°50'24"W	16.5
Bruin	Pinckney	Washtenaw	42°25'07"N, 84°02'23"W	14.5
Cedar	Waterloo	Washtenaw	42°18'52"N, 84°04'45"W	7
Crooked P	Pinckney	Washtenaw	42°25'11"N, 83°58'57"W	12
Crooked W	Waterloo	Washtenaw	42°19'32"N, 84°06'43"W	6
Gosling	Pinckney	Livingston	42°26'22"N, 84°00'12"W	6
Little Appleton	Brighton	Livingston	42°30'24"N, 83°50'19"W	6
Mill	Waterloo	Washtenaw	42°19'46"N, 84°05'27"W	6
North	Pinckney	Washtenaw	42°23'35"N, 84°00'23"W	17
Pickerel	Pinckney	Washtenaw	42°24'37"N, 83°58'58"W	16
Sullivan	Pinckney	Washtenaw	42°23'55"N, 84°03'25"W	6.5
Walsh	Waterloo	Washtenaw	42°20'15"N, 84°04'4"W	6
Whitmore	Brighton	Livingston & Washtenaw	42°25'42"N, 83°45'08"W	19.5
Woodland	Brighton	Livingston	42°33'12"N, 83°46'29"W	10.5

962

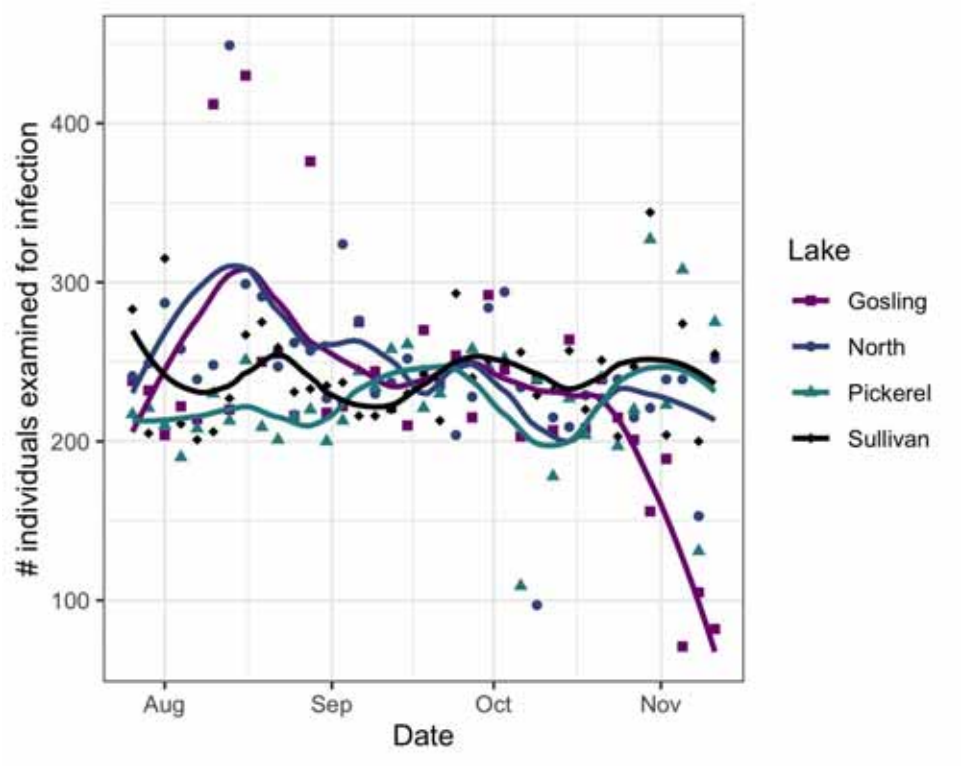

Figure S3. Number of *D. dentifera* individuals that were examined for infection on each date in the four study lakes.

Table S2. List of genomic data used for the phylogenomic analysis

Genus	Species	Strain	Source	Accession
Ordospora	pajunii	MicG	JGI	
Ordospora	pajunii	FI-F-10	NCBI	GCA_021821965.1
Ordospora	colligata	OC4	NCBI	GCA_000803265.1
Ordospora	colligata	GB-EP-1	NCBI	GCA_004324935.1
Ordospora	colligata	FI-SK-17-1	NCBI	GCA_004325055.1

Ordospora	colligata	NO-V-7	NCBI	GCA_004324945.1
Encephalitozoon	cuniculi	GB-M1	NCBI	GCA_000091225.2
Encephalitozoon	intestinalis	ATCC50506	NCBI	GCA_000146465.1
Encephalitozoon	romaleae	SJ-2008	NCBI	GCA_000280035.2
Encephalitozoon	hellem	ATCC50504	NCBI	GCA_000277815.3
Nosema	apis	BRL01	NCBI	GCA_000447185.1
Nosema	ceranae	BRL	NCBI	GCA_004919615.1
Nosema	bombycis	CQ1	NCBI	GCA_000383075.1
Nosema	granulosis	Ou3-Ou53	NCBI	GCA_015832245.1
Enterospora	canceri	GB1	NCBI	GCA_002087915.1
Enterocytozoon	bieneusi	H348	NCBI	GCA_000209485.1
Enterocytozoon	hepatopenaei	CIBAehp1	NCBI	GCA_026692725.1
Hepatospora	eriocheir	GB1	NCBI	GCA_002087885.1
Vittaforma	corneae	ATCC50505	NCBI	GCA_000231115.1
Anncaliia	algerae	PRA339	NCBI	GCA_000385875.2
Edhazardia	aedis	USNM41457	NCBI	GCA_000230595.3
Tubulinosema	ratisbonensis	Franzen	NCBI	GCA_004000155.1
Thelohania	contejeani	T1	NCBI	GCA_014805555.1

Hamiltosporidium	magnivora	BE-OM-2	NCBI	GCA_004325065.1
Hamiltosporidium	tvaerminnensis	FI-OER-3-3	NCBI	GCA_022605425.1
Cucumispora	dikerogammari	Dv6	NCBI	GCA_014805705.1
Spraguea	lophii	Celtic_Deep	NCBI	GCA_001887945.1
Trachipleistophora	hominis		NCBI	GCA_000316135.1
Vavraia	culicis	floridensis	NCBI	GCA_000192795.1
Pseudoloma	neurophilia	MK1	NCBI	GCA_001432165.1
Nematocida	displodere	JUm2807	NCBI	GCA_001642395.1
Nematocida	parisii	ERTm1	NCBI	GCA_000250985.1
Nematocida	ausubeli	ERTm6	NCBI	GCA_000738915.1
Nematocida	ironsii	ERTm5	NCBI	GCA_001642415.1
Dictyocoela	roeselum	Ou19	NCBI	GCA_016255985.1
Dictyocoela	muelleri	Ou54	NCBI	GCA_016256075.1
Antonospora	locustae	CLX	NCBI	GCA_007674295.1
Amphiamblys	sp.	WSBS2006	NCBI	GCA_001875675.1
Metchnikovella	incurvata	LNA5	NCBI	GCA_003600395.1

980 **Host range**

981 **Table S3.** Proportion of clone S and *D. longispina* clones displaying visible infection.

982

Genotype	Proportion Infected
S	1
OLCH 17	0
STEC 8	0
STEC 49	0.8
WALD 12	0
WALD 37	0.9

983

984